Supplementary materials

1. EV initial structure:

Generating an initial stable EV structure for molecular dynamics simulations is crucial in accurately studying EVs and their behavior. While there are multiple methods for generating EV structures, one widely adopted approach involves utilizing an in-house script to create the EV and then equilibrating it to achieve stability.

The initial creation of the EVs involves carefully placing the lipid molecules in a periodic box and arranging them in a bilayer configuration while aligning the tails with the head of the lipid and maintaining a constant distance between the head groups. Following this, the EV is subjected to equilibration, which allows it to relax and attain a stable configuration. Equilibration is a fundamental step in the process, as it involves simulating the EV under conditions that allow for relaxation and equilibrium. We enable the initial structure to be equilibrated using a Langevin thermostat while closely monitoring the fluctuations in shape, size, and orientation of the lipids, and the simulation is run for a sufficient amount of time until a stable liposome configuration is obtained.

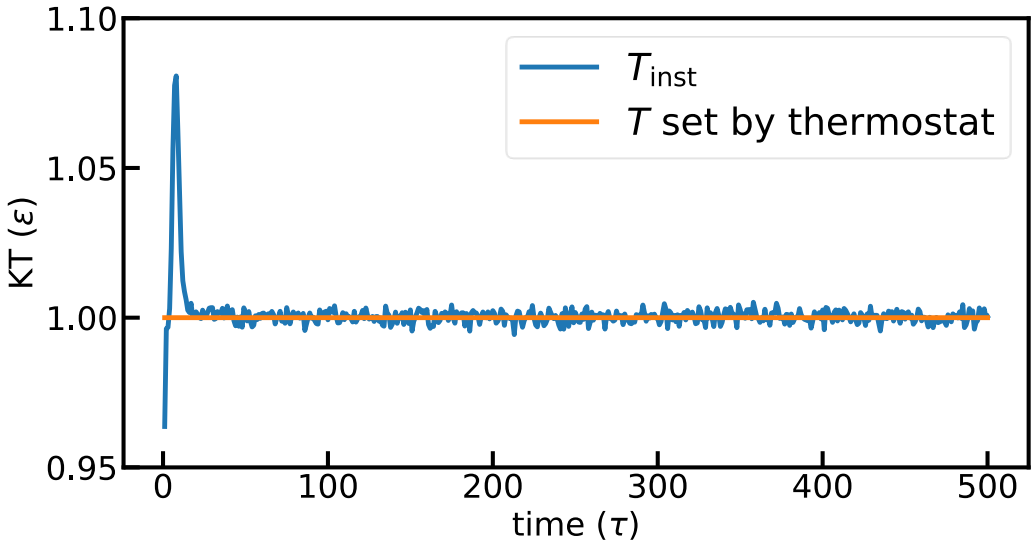

Figure S1: Temperature fluctuation over time

In Figure S1, we can observe the temperature fluctuations over time. The temperature visualization includes two distinct colors to differentiate between the instantaneous temperature and the temperature the thermostat defines. Blue represents the instantaneous temperature, while orange represents the temperature specified by the thermostat. The figure clearly shows that the temperature initially spiked up at the very beginning of the simulation. This spike can be attributed to the unstable initial structure manually created using our script. However, it's important to note that this spike was quickly brought down to the desired temperature by implementing the Langevin thermostat. The Langevin thermostat is a widely used method to control the temperature in molecular dynamics simulations by mimicking the effect of a heat bath on the system. With the Langevin thermostat, the temperature was tabilized and fluctuated around the set temperature. This fluctuation is natural, as expected, and indicates that the simulation is proceeding with a minimized stable configuration.

2. Velocity profile:

In our simulation, Poiseuille flow is generated by specifying uniform force per unit of volume. By carefully adjusting the applied force, we have achieved the desired maximum velocity at the center of the channel. Our simulation results are presented in Figure S2, which clearly visualizes the fluid velocity profile at various flow conditions. The velocity profile is obtained by employing a polynomial fit to the fluid velocity data along the x direction. Our graph illustrates the gradual increase of velocity along the constriction region, where it reaches a maximum value, followed by a gradual decrease to a minimum value in the remaining parts of the channel. This detailed representation of the velocity profile provides valuable insights into the Poiseuille flow behavior within the nanochannel.

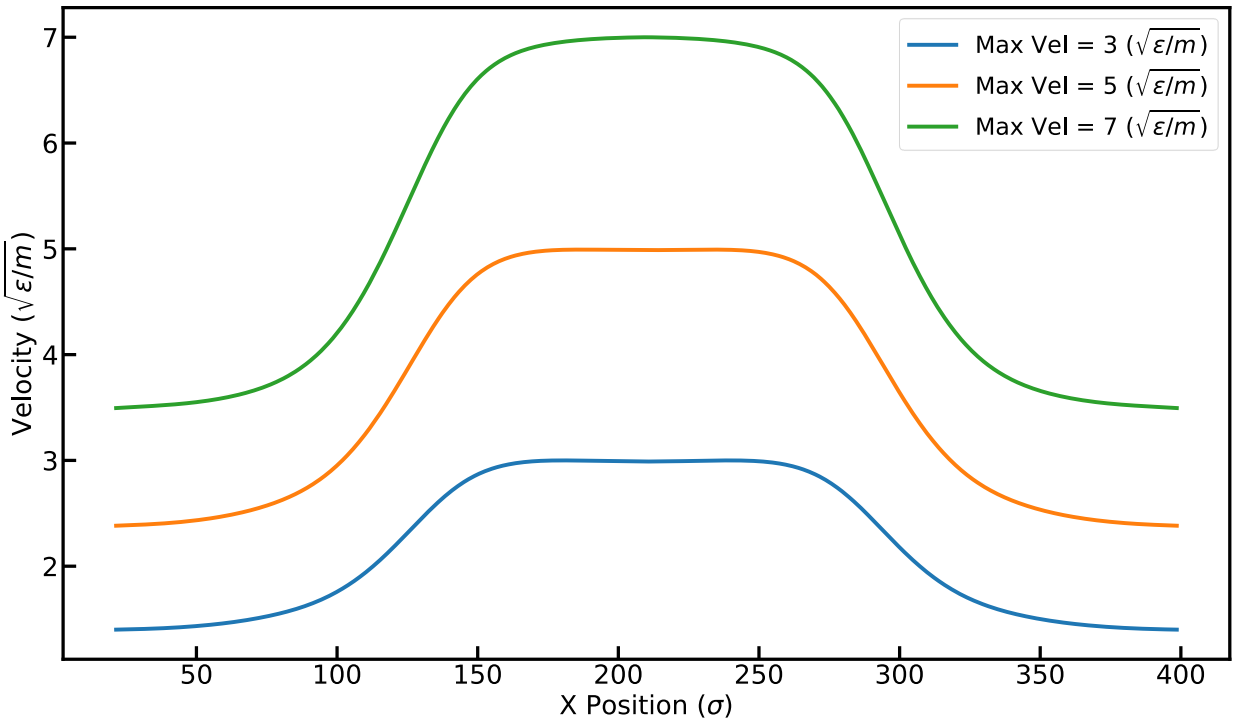

Figure S2: Fluid velocity profile over different regions of the nanochannel

3. EV damage criteria:

Extracellular vesicle (EV) being a subtype of extracellular vesicle and made of lipid-bilayer nanoscale membrane particles (one head and two tails), we believe the damage of EV should follow similar failure criteria as a standard biological membrane. Literature review [1–3] reveals that bilayer membrane ruptures are prone to occur between tension ~1-25 mN/m, which corresponds to strain value in the order of 2 -5%. Evans et al [4] found two distinct regimes for rupture: low-strength cavitation-limited and a high-strength defect-limited regime with a transition at loading rate(tension/time) for DOPC bilayer membrane around 10 mN/m/s. They show that membrane failure is not a static material property but a function of dynamic loading. Membrane tension can vary from 6 mN/m to 13 mN/m for loading rates of 0.07 mN/m/s and 25 mN/m/s respectively. Our squeezing simulation of EVs through nanochannel causes the EV to be damaged. Zevnik[5] et al. show

through simulation that for a high loading rate in the range of ~ 10^9 – 10^{10} mN/m/s critical rupture strength rises logarithmically and stays between 80 to 95 mN/m. Their results closely mimic the molecular dynamics simulation of liquid-phase DPPC bilayer[6]. Based on the values from the literature, we considered two criteria for EV damage. The primary damage criterion is the areal strain value of 0.203 and the secondary damage criterion is the aggregation of pores.

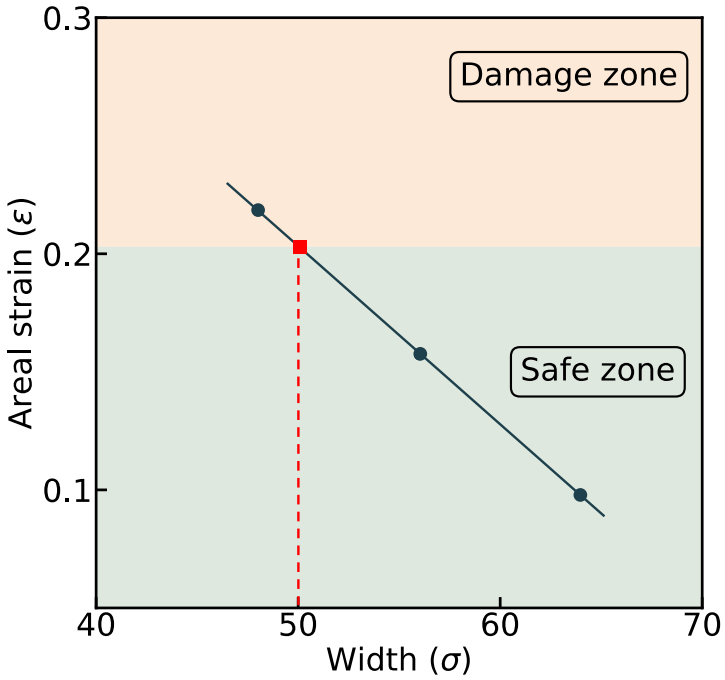

Figure S3: Safe vs damage zone of EV for change of width case

Primary damage criteria:

The primary cause of EV membrane damage is the creation of pores caused by squeezing the EV through the nanochannel. Zevnik et al. [5] show that for an equibiaxial loading case, the critical stress value is 20MPa. Although the pore formation and subsequent EV damage largely depend on the strength of the membrane here, we consider a critical areal strain of value 0.203 calculated from obtained linear strain by Zevnik et al. [5].

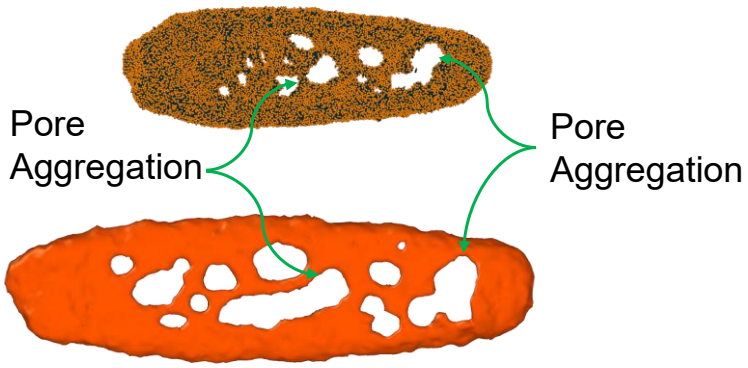

Figure S4: Pore aggregation for $W_1 = 0.6D$ case

Secondary damage criteria:

The secondary cause of EV damage is due to aggregation of pores. If two or more pore aggregate together, it creates a massive irregular-shaped pore in the membrane, potentially damaging the cell. The aggregation of pores is inspected after constructing the surface mesh, as described in section 2.2 of the paper. Most of the single pore is roundish in shape if no pore aggregation happens.

As shown in figure S1, the threshold areal strain value of .203 divides the graph into the damage zone and safe zone. The first case from the width change fulfils both criteria to be considered a damaged EV case. Figure S1 shows the areal strain for various constriction width cases. Areal strain for width $W_1 = 0.6D$ is calculated as 0.218, above our estimated threshold value of 0.203 and falls in the EV damage zone. A trend line is drawn connecting the three data points, and the intersecting point between the threshold value and the trendline is marked with a red box. The intersection point is then extrapolated towards the x-axis to get the desired minimal channel width value to achieve maximum exosomal pore without damaging the EV. Figure S2 shows the aggregation of pores with surface representation as described in section 2.2 of the paper. The pore aggregates as the exos EV ome propagate along the flow direction, creating a larger irregular-shaped pore.

References:

(1) Olbrich, K.; Rawicz, W.; Needham, D.; Evans, E. Water Permeability and Mechanical Strength of Polyunsaturated Lipid Bilayers. *Biophys J* **2000**, *79* (1), 321–327. https://doi.org/10.1016/S0006-3495(00)76294-1.

(2) Rawicz, W.; Olbrich, K. C.; McIntosh, T.; Needham, D.; Evans, E. A. Effect of Chain Length and Unsaturation on Elasticity of Lipid Bilayers. *Biophys J* **2000**, *79* (1), 328–339. https://doi.org/10.1016/S0006-3495(00)76295-3.

(3) Barton, P. G.; Gunstone, F. D. Hydrocarbon Chain Packing and Molecular Motion in Phospholipid Bilayers Formed from Unsaturated Lecithins. Synthesis and Properties of Sixteen Positional Isomers of 1,2 Dioctadecenoyl Sn Glycero 3 Phosphorylcholine. *Journal of Biological Chemistry* **1975**, *250* (12), 4470–4476. https://doi.org/10.1016/s0021-9258(19)41327-6.

(4) Evans, E.; Heinrich, V.; Ludwig, F.; Rawicz, W. Dynamic Tension Spectroscopy and Strength of Biomembranes. *Biophys J* **2003**, *85* (4), 2342–2350. https://doi.org/10.1016/S0006-3495(03)74658-X.

(5) Zevnik, J.; Dular, M. Liposome Destruction by a Collapsing Cavitation Microbubble: A Numerical Study. *Ultrason Sonochem* **2021**, *78*. https://doi.org/10.1016/j.ultsonch.2021.105706.

(6) Leontiadou, H.; Mark, A. E.; Marrink, S. J. Molecular Dynamics Simulations of Hydrophilic Pores in Lipid Bilayers. *Biophys J* **2004**, *86* (4), 2156–2164. https://doi.org/10.1016/S0006-3495(04)74275-7.